Biochimica et Biophysica Acta 1864 (2016) 1775–1786

Contents lists available at ScienceDirect

Biochimica et Biophysica Acta

journal homepage: www.elsevier.com/locate/bbapap

Exposure of cultured fibroblasts to the peptide PR-11 for the identification of induced proteome alterations and discovery of novel potential ligands

Gustavo Silveira Breguez [a], Leandro Xavier Neves [b], Karina Taciana Santos Silva [c], Lorran Miranda Andrade de Freitas [a], Gabriela de Oliveira Faria [a], Mauro César Isoldi [d], William Castro-Borges [d], Milton Hércules Guerra de Andrade [d,*]

[a] Programa de Pós-Graduação em Ciências Biológicas, Universidade Federal de Ouro Preto, Ouro Preto, Minas Gerais, Brazil
[b] Programa de Pós-Graduação em Biotecnologia, Universidade Federal de Ouro Preto, Ouro Preto, Minas Gerais, Brazil
[c] Departamento de Farmácia, Universidade Federal de Ouro Preto, Ouro Preto, Minas Gerais, Brazil
[d] Departamento de Ciências Biológicas, Núcleo de Pesquisas em Ciências Biológicas, Universidade Federal de Ouro Preto, Ouro Preto, Minas Gerais, Brazil

ARTICLE INFO

Article history:
Received 11 May 2016
Received in revised form 7 September 2016
Accepted 26 September 2016
Available online 28 September 2016

Keywords:
PR-39
PR-11
Proline rich-peptides
Label-free shotgun
PR-11 binding proteins

ABSTRACT

The PR-11 peptide corresponds to the N-terminal and active region of the endogenously synthesized PR-39 molecule, of porcine origin. It is known to possess various biological effects including antimicrobial properties, angiogenic and anti-inflammatory activities. Apart from its reported activity as a proteasome inhibitor, a more comprehensive understanding of its function, at the molecular level, is still lacking. In this study, we used a label-free shotgun strategy to evaluate the proteomic alterations caused by exposure of cultured fibroblasts to the peptide PR-11. This approach revealed that more than half of the identified molecules were related to signalling, transcription and translation. Proteins directly associated to regulation of angiogenesis and interaction with the hypoxia-inducible factor 1-α (HIF-1α) were significantly altered. In addition, at least three differentially expressed molecules of the NF-κB pathway were detected, suggesting an anti-inflammatory property of PR-11. At last, we demonstrated novel potential ligands of PR-11, through its immobilization for affinity chromatography. Among the eluted molecules, gC1qR, a known complement receptor, appeared markedly enriched. This provided preliminary evidence of a PR-11 ligand possibly involved in the internalization of this peptide. Altogether, our findings contributed to a better understanding of the cellular pathways affected by PR-39 derived molecules.

1. Introduction

The peptide PR-11, a ~1.4 kDa molecule highly rich in proline and arginine residues, corresponds to the N-terminal active region of PR-39, the latter formerly isolated from the small intestine [1] and bone marrow of pigs [2]. PR-39 acts against a wide spectrum of bacteria, including clinical isolates resistant to multiple drugs [3,4]. At micromolar concentrations, the peptide is rapidly internalized and interferes with various cellular processes such as inhibition of DNA synthesis and translation. At higher levels, a bactericide activity is also observed, possibly by perturbation of cell membrane stability [5,6]. Aside from its antimicrobial properties, PR-39 stimulates neutrophil migration [7], inhibits apoptosis [8–10] and reduces motility and cell proliferation in cancer tissues [11,12].

PR-39 has been shown to bind intracellular SH3 domain-containing proteins [13] and its role as a proteasome regulator also reported. The hypoxia signalling and NF-κB pathways are known to be compromised by PR-39 proteasome-dependent inhibition resulting in angiogenic [14] and anti-inflammatory effects [15,16], respectively. Sequential C-terminal residue deletions of PR-39 in parallel to evaluation of the resulting activity over the 20S proteasome, revealed the requirement of at least 11 N-terminal amino acids to sustain its inhibitory property, in a dose-dependent manner [17]. Atomic force microscopy also demonstrated that upon binding of PR-39 and PR-11 to 26S and 20S proteasomes, their cylindrical architecture is reversibly altered [17].

Given the wide repertoire of biological activities of PR-39 and PR-11 and the limited knowledge of their interfering molecular pathways, we used a label-free shotgun approach to evaluate the proteome alterations caused by exposure of cultured fibroblasts to 1 μM PR-11. Our findings demonstrated that >50% of the identified differentially expressed proteins are related to cell signalling, transcription and translation. In addition, using immobilized PR-11 affinity chromatography, we were

* Corresponding author.
E-mail address: miltonguerra00@gmail.com (M.H.G. de Andrade).

http://dx.doi.org/10.1016/j.bbapap.2016.09.017
1570-9639/

able to identify novel potential ligands, providing a better understanding of its mechanism of action.

2. Materials and methods

2.1. Ethics statement

The procedures involving animals were carried out in accordance with the Brazilian legislation (11790/2008). They were reviewed and approved by the local ethics committee on animal experimentation (CEUA), Universidade Federal de Ouro Preto (UFOP), and received the protocol number 2013/09.

2.2. Synthesis of the PR-11 peptide

PR-11 peptide was chemically synthesized based on the amino acid composition of the 11 N-terminal residues (RRRPRPPYLPR) of PR-39. PR-11 was purified by HPLC using reversed-phase chromatography (Shimadzu Scientific Instruments) (Supplementary Fig. 1), identified by direct injection in an IT-TOF mass spectrometer (Shimadzu Scientific Instruments) and finally reconstituted in water. Peptide concentration was calculated using the molar extinction coefficient at 280 nm of its constituent tyrosine residue (1280 M^{-1} cm^{-1}).

2.3. Fibroblasts culture and exposure to PR-11 peptide

Fibroblasts were obtained from lungs of neonate Wistar rats, aged 2 days and of approximately 5 g weight. Briefly, after removal of the lungs, these were washed in 1× ADS buffer (115 mM NaCl; 20 mM Hepes, 1 mM Na_2HPO_4, 5 mM D-glucose; 5 mM KCl; 1.6 mM $MgSO_4$) and subjected to 3 cycles of digestion with 0.8 mg/mL pancreatin (Sigma-Aldrich) for 20 min at 37 °C. Cells were recovered by centrifugation at 1.000 ×*g* for 10 min and resuspended in DMEM medium supplemented with 15% v/v fetal bovine serum and 1% v/v penicillin/streptomycin. Prior to exposure of cells to PR-11, a minimum cell confluence of >90% throughout the well was required under microscopic observation and the supernatant should contain a negligible number of detached cells. Primary fibroblast cultures (unique passage) were exposed to 1 μM PR-11 during 2, 6 and 10 h. Control cultures, in which water was added instead of the water-soluble peptide, were obtained for the same time points. At the end of the incubation periods, the supernatant containing PR-11 peptide was completely removed and the cells were gently detached from the wells using the TrypLE reagent (Gibco). These were finally recovered by centrifugation. The experiments were performed in biological triplicates.

2.4. Soluble protein extract and in solution digestion

Control and treated fibroblasts were resuspended in 500 μL of 25 mM Tris-HCl pH 7.5; 1 mM DTT and 1% v/v glycerol buffer containing 1× protease inhibitor cocktail (Sigma-Aldrich). Samples were sonicated on ice through 4 cycles of 20 pulses each, with 45 s rest between cycles. The homogenates were centrifuged at 100,000 ×*g* for 1 h and the protein concentration determined by BCA method (Thermo Scientific).

Soluble proteins present in a 20 μg aliquot were reduced using 4 mM dithiothreitol (Sigma-Aldrich) in 100 mM ammonium bicarbonate at 56 °C for 15 min and then alkylated in 8 mM iodoacetamide (Sigma-Aldrich) for 15 min in the dark. Enzymatic digestion was carried out at 37 °C for 18 h using 0.8 μg Sequencing Grade Modified Trypsin (Promega) and the reaction was interrupted by acidification with 10 μL acetic acid. Tryptic peptides were cleaned up using a Strata C18-E cartridge (55 μm, Phenomenex), dried over speed vacuum and resuspended in 0.1% v/v formic acid.

2.5. Mass spectrometry analysis: in solution digestion

For each sample, 3 μg of tryptic peptides were separated in a UltiMate® 3000 UHPLC system (Thermo Scientific) equipped with a C18 column (PepMap Acclaim RSLC — 75 nm × 15 cm, Thermo Scientific) under mobile phase flow of 0.3 μL/min using a nonlinear gradient (4 to 90% of 80% *v*/v acetonitrile and 0.1% v/v formic acid) during 180 min. The eluted peptides were ionized in a ESI-nanospray interface and analyzed in a Q-Exactive™ Hybrid Quadrupole-Orbitrap instrument (Thermo Scientific) under the acquisition mode Full MS followed by MS/MS. The following operating parameters were set: Full MS resolution: 70.000; MS/MS resolution: 17,500; scan range: 300–2000 *m*/*z*; 12 most abundant isotope patterns scanned; loop count: 10; isolation window: 2.0 *m*/*z*; ions exhibiting charge +2, +3 or +4; dynamic exclusion: 60 s; positive ionization mode.

The Xcalibur v.3.0.63.3 and MaxQuant v.1.5.2.8 softwares [18] were used for the acquisition and data analysis, respectively. Database searches were performed using a UniProt *Rattus norvegicus* compilation containing 30,091 sequences. Search parameters included: enzyme: trypsin/P; carbamidomethylation of cysteine as fixed modification; oxidation of methionine and N-terminal acetylation as variable; maximum missed cleavage sites: 2; mass tolerance: 4.5 ppm; isotope match tolerance: 2 ppm; minimum peak length: 2; False Discovery Rate (FDR) and Peptide Sequence Match (PSM): 0.01; minimum ratio count: 2. Relative abundance of proteins were obtained using Label-Free Quantification (LFQ) provided by the LFQ intensity data (unique + razor peptides).

2.6. Statistical analyses and protein functional categorization

Statistical analysis was performed using the Graph Pad Prism software v.6.01. For each exposure time to the PR-11 peptide, proteins exhibiting at least two LFQ intensity data among the three biological triplicates were regarded genuine identifications. These were subjected to a *t*-test and the proteins with $p < 0.01$ were considered significantly altered. Differentially expressed proteins were categorized using the UniProtKB database (available at www.uniprot.org) according to their biological functions.

2.7. Total protein extraction, affinity chromatography and in gel digestion

A liver protein extract from Wistar rat was obtained for use in immobilized PR-11 affinity chromatography. Approximately 100 mg tissue section was homogeneized in 1 mL of extraction buffer (50 mM Tris-HCl pH 7.5; 100 mM NaCl) containing 1× protease inhibitor cocktail (Sigma-Aldrich). Sample was sonicated on ice through 5 cycles of 20 pulses each, with 45 s rest between cycles. The homogenate was centrifuged at 20,000 ×*g* for 1 h and the protein concentration determined by BCA method (Thermo Scientific).

Coupling of PR-11 peptide to the Sepharose 4B matrix was performed as previously described [19]. Approximately 10 mg of total proteins were loaded onto a 1 mL column containing immobilized PR-11. The column was extensively washed with 50 mM Tris-HCl pH 7.5; 300 mM NaCl and 5 mM $MgCl_2$ and the bound fraction recovered after loading 1 mL of 50 μM PR-11. The collected samples were dialyzed in 10 mM ammonium acetate pH 7.4 and dried over speed vacuum. Aliquots taken from the collected samples were analyzed under denaturing conditions using 12% SDS-PAGE as classically described [20] and the gel stained in silver nitrate.

Visualized bands from the bound fraction were excised manually for in gel digestion. The bands were destained in 0.5% w/v potassium ferricyanide/10% w/v sodium thiosulfate and washed in 40% v/v ethanol/7% v/v acetic acid. Disulfide bonds were reduced in 500 μL of 50 mM DTT at 65 °C for 30 min and alkylated in 300 μL of 100 mM iodoacetamide at room temperature for 1 h in the dark. Gel pieces were washed in 500 μL of 20 mM NH_4HCO_3/50% v/v acetonitrile for 3 × 20 min and dried in a speed vacuum. Then, gel pieces were rehydrated in 20 μL of

0.033 μg/μL Sequencing Grade Modified Trypsin (Promega) in 20 mM NH_4HCO_3. Trypsin digestion proceeded at 37 °C for 18 h. For each sample, the resulting peptides were recovered, dried over speed vacuum and resuspended in 10 μL of 0.1% formic acid.

2.8. Mass spectrometry analysis: in gel digestion

Tryptic peptides from each band were loaded onto a UltiMate® 3000 UHPLC system (Thermo Scientific) equipped with a C18 column (PepMap Acclaim RSLC — 75 nm × 15 cm, Thermo Scientific). A nonlinear gradient was set to 4–90% of 80% v/v acetonitrile in 0.1% v/v formic acid during 45 min under a flow rate of 0.3 μL/min. The eluted peptides were ionized in a ESI-nanospray interface and analyzed in a Q-Exactive™ Hybrid Quadrupole-Orbitrap instrument (Thermo Scientific) under the acquisition mode Full MS followed by MS/MS. The following operating parameters were set: Full MS resolution: 70.000; MS/MS resolution: 17.500; scan range: 300–2000 *m/z*; 10 most abundant isotope patterns scanned; loop count: 10; isolation window: 2.0 *m/z*; ions exhibiting charge +2, +3 or +4; dynamic exclusion: 90 s; positive ionization mode.

The Xcalibur v.3.0.63.3 and Proteome Discoverer v.1.5.2.8 softwares were used for acquisition and data analysis, respectively. Database searches were performed using a UniProt *Rattus norvegicus* reviewed compilation containing 9584 sequences. Search parameters included: enzyme: trypsin/P; carbamidomethylation of cysteine as fixed modification; oxidation of methionine and N-terminal acetylation as variable; one miscleavage site; mass tolerance: 10 ppm and 0.1 Da to MS and MS/MS, respectively; peptide mass: 300–4000 Da; high peptide confidence; at least 3 unique peptides per identified protein; quantification by area detector. A minimum of 10% contribution to the total area detected in each band was required to assign a protein identity.

3. Results

3.1. Label-free quantitative proteomics

Shotgun analyses of the soluble fractions, from cultured fibroblasts exposed to 1 μM PR-11 for 2, 6 and 10 h, revealed a total of 1941 molecules confidently identified in at least one of the three timing points (Supplementary Table 1). Using the LFQ intensity data, a Spearman correlation analysis was conducted to assess sample reproducibility in the three independent biological replicates. As shown in Supplementary Fig. 2, correlation coefficients varied from 0,917 to 0,980, indicating that samples were suitable for downstream comparative analyses. Then, by applying a stringent criteria for quantification of differentially expressed proteins ($p < 0,01$), it was found 57, 67 and 59 molecules significantly altered in PR-11 exposed fibroblasts treated for 2, 6 and 10 h, respectively (Fig. 1). After 2 h exposure, 26 proteins were downregulated, whilst 31 were at increased levels relative to untreated cells. At 6 h post exposure, both the number of down- and upregulated molecules increased to 29 and 38, respectively. At 10 h, 2/3 of the differentially expressed proteins (39) were downregulated and the remaining (20) was found at increased levels. Of note, according to our statistic criteria for quantification the differentially expressed proteins were mostly unique to each time point, as shown in Fig. 2. Although 1388 (71,5% of the total) proteins were commonly identified in the three time points (Fig. 2A), only seven shared identities appeared differentially expressed (Fig. 2B).

3.2. Categorization of differentially expressed proteins

All 175 differentially expressed proteins ($p < 0,01$) were classified according to their biological function into 9 distinct categories using UniProtKB annotation, Fig. 3 and Table 1. Over 50% of the categorized proteins are involved with cell signalling (74) and transcription/translation (33). Out of 59 differentially expressed proteins found at 2 h, 17

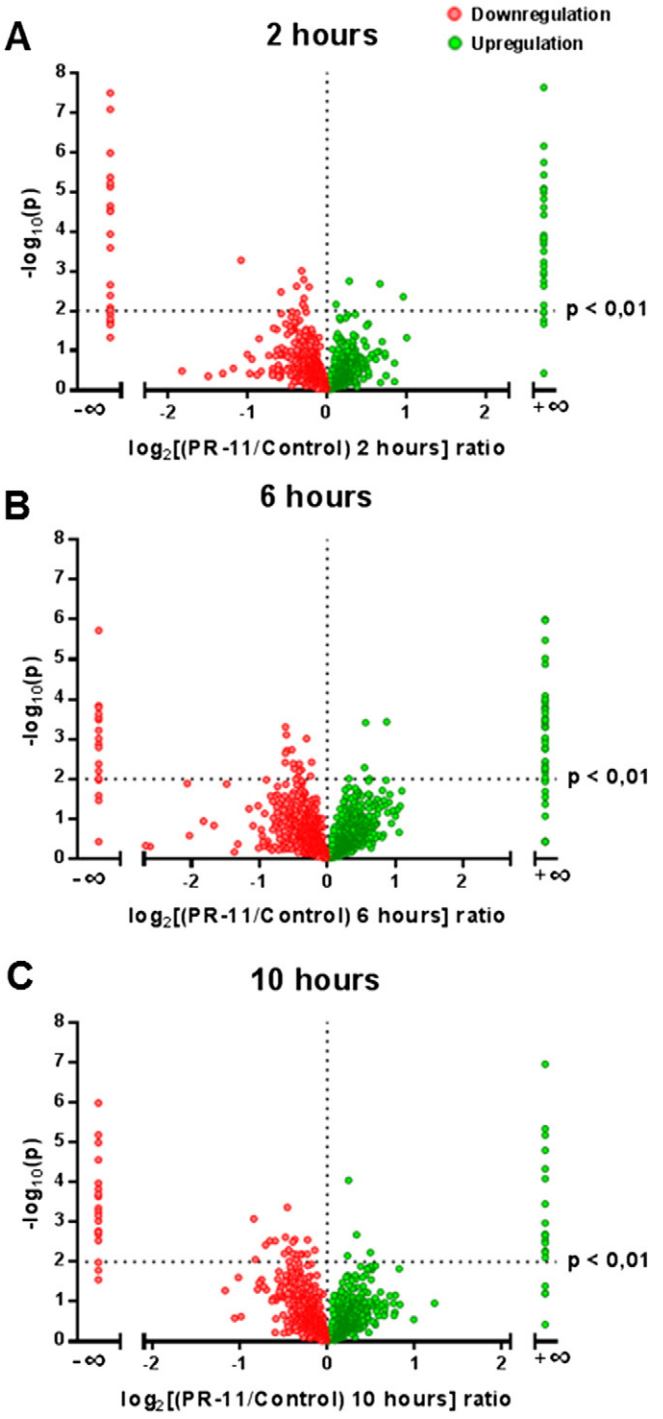

Fig. 1. Volcano plots revealed similar distribution of down- and upregulated molecules throughout the three timing points. A–C: Protein expression in fibroblasts exposed to 1 μM PR-11 during 2, 6 and 10 h measured by fold (±) and *p* value. Differentially expressed proteins ($p < 0,01$) are exhibited above the dashed horizontal line. Proteins detected only in untreated cells or exposed fibroblasts are displayed above fold infinity (±). Median folds were obtained using the three independent biological triplicates.

were unique from untreated cells whilst 27 were found in PR-11 exposed fibroblasts. At this time point, proteins exhibiting the most altered levels were mitochondrial fission 1 protein (0,47 fold – cell signalling), the translation initiation factor eiF2B subunit delta (1,59 fold – transcription/translation) and nucleoporin 85 kDa (1,95 fold – structural).

At 6 h post exposure, out of 67 molecules significantly altered, 14 and 33 proteins were found only in control or treated fibroblasts,

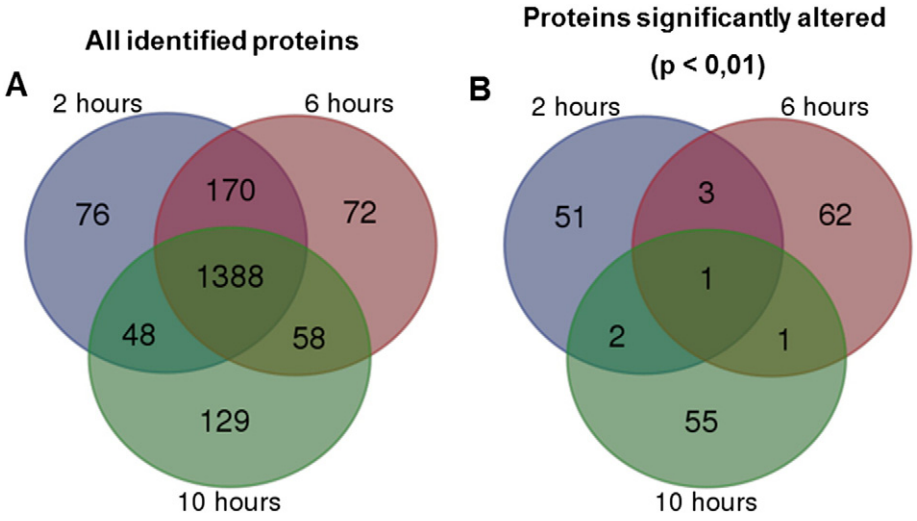

Fig. 2. Fibroblasts exposed to the PR-11 peptide display time-dependent proteomic alterations. A: In total, 1388 or 71,5% of the proteins were identified in the three timing points. B: Only seven shared identities appeared differentially expressed among all exposure times.

respectively. Cell signalling category had the highest number of altered proteins (29), highlighting the downregulation of vesicle trafficking 1, SEC23 homolog B (0,65 fold), RACK1 and SEC24 homolog D (0,66 fold) and the upregulation of CGR11 (1,83 fold), R-ras (1,48 fold) and 14–3-3 protein beta/alpha (1,46 fold). Transcription/translation was the second category containing a significant number of altered proteins. In particular, decreased levels for 4 quantified proteins – acinus, 40S ribosomal protein S4, hnRPN D and the translation elongation factor eEF1B2 (0,75; 0,75; 0,77 and 0,81) – were observed. In the group of structural proteins, mitochondrial inner membrane protein (0,65 fold) and transgelin-2 (1,25 fold) were the two molecules showing the most pronounced alterations.

After 10 h exposure, 19 out of 39 significantly downregulated proteins were found only in untreated fibroblasts, whilst 16 out of 20 from PR-11 exposed cells exhibited increased levels. Exportin-2 (0,56 fold), ataxin-10 (0,57 fold) and cysteine and glycine-rich protein 1 were the most altered cell signalling representatives. Within transcription/translation category, out of 11 molecules differentially expressed, SFRS7 was the unique quantified protein in both treated and untreated cells (1,17 fold).

3.3. Identification of PR-11 binding proteins

A liver protein extract from Wistar rat was loaded onto an immobilized PR-11 affinity chromatography. Unspecific binding was addressed by applying a stringent washing step (300 mM NaCl). This procedure intended to disrupt electrostatic interactions and removal of bound proteins with low affinity to the column. After exhaustive washing steps, one column volume was dried to completion and analyzed by SDS-PAGE. Silver staining on the gel revealed no protein band (Fig. 4, FPE: fraction prior to elution). Elution of bound material was performed using 50 μM PR-11. 12% SDS-PAGE allowed the visualization of 9 bands in the eluted fraction (Fig. 4, EF: eluted fraction). These were successfully identified by mass spectrometry (Table 2). Of particular interest, band 7 contained a dominant constituent (relative area detector: 96.2%) identified as the gC1qR protein. 78 kDa glucose-regulated protein (band 2), ornithine carbamoyltransferase (band 6) and carbonic anhydrase 3 (band 8) were also prominent in their respective bands contributing to at least 65% of the relative area detected.

4. Discussion

In this study we seek to investigate the soluble proteome alterations caused by exposure of fibroblasts to the peptide PR-11 to gain further understanding of its biological functions. Knowledge of its angiogenic and anti-inflammatory properties makes PR-11 of particular interest for specific processes, such as wound repair *via* topic administration or infused through different routes. In the present work, micromolar concentration was employed to account for PR-11 peptide degradation or limited absorption. The choice of the micromolar range has been also reported by other studies that used PR-39 derived molecules in cell cultures or distributed through tissues [15,21].

By combining improved resolution for chromatographic separation of peptides and increased accuracy of modern mass spectrometry instrumentation [22,23] we were able to identify and quantify almost two thousand soluble proteins, using a label-free shotgun approach. The statistical analysis was performed as described by the inventors of the MaxQuant software [18], in which a standard *t*-test is employed. This test was used to measure minor alterations in protein levels in this first global analysis of proteome alterations induced by the PR-11 peptide. A more stringent condition of analysis could mask some real and existing alterations. The detected protein abundance differed in five orders of magnitude, allowing for quantitative evaluation of proteomic alterations among major and minor components of our protein preparation. The volcano plots displayed a similar distribution of up- and downregulated molecules throughout the three timing points. Nevertheless, analysis of the Venn diagram demonstrates unique proteome alterations caused by PR-11 at the different sampling times, relative to the respective non-exposed control cells, possibly reflecting cell-stage specific proteins altered by the treatment.

In total, 175 molecules were found at increased or decreased levels over the 10 h experiment. Protein categorization, using biological function, revealed that over 40% is represented by molecules involved in cell signalling. In fact, PR-39 and PR-11 are known to interfere with important cellular pathways such as the hypoxia-inducible factor 1-α (HIF-1α) [14] and nuclear factor kappa B (NF-κB) [15,16]. Here we proposed to initiate the discussion of our findings in the context of these two signalling events to give mechanistic insights into the putative roles of PR-11 in cell biology.

- Hypoxia-inducible factor-1 α pathway

The peptides PR-39 and PR-11 are able to stimulate angiogenesis both *in vitro* and *in vivo* [16,17]. Studies have shown that the transient expression of PR-39 in cardiomyocytes resulted in increased vascularization, reduced resistance to blood flow and myocardial hypertrophy [14,24,25]. These effects are partially explained by decreased proteasomal degradation of HIF-1α, a molecule known to regulate the expression of several genes related to angiogenesis, including VEGF

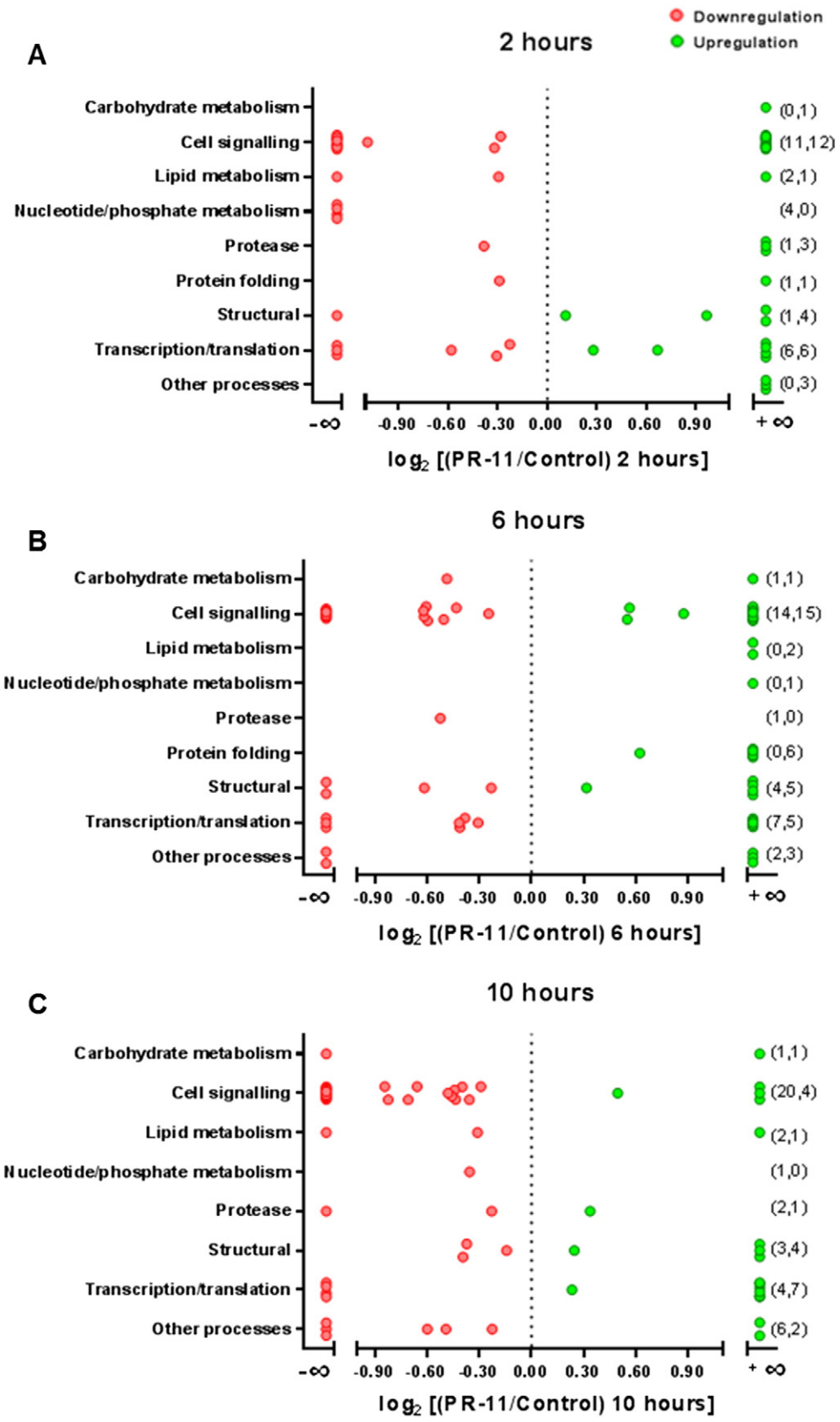

Fig. 3. Functional classification of differentially expressed proteins from cultured fibroblasts exposed to 1 μM PR-11 for 2, 6 and 10 h. A-C: Proteins significantly altered ($p < 0,01$) were categorized according to their biological function into 9 distinct categories using UniProtKB annotation. Measurements of down- or upregulation of proteins in each category are indicated by numbers in parentheses, respectively. Of note, over half of the classified proteins are associated with cell signalling (74) and transcription/translation (33).

Table 1
Classification of differentially expressed proteins ($p < 0,01$) according their biological function (UniProtKB annotation).

2 h						
ID UniProtKB	Protein	Gene	PR-11/Control ratio	p value	Razor + unique peptides	Unique + razor coverage [%]
Carbohydrate metabolism						
Q02401; A9CMC8	Lactase-phlorizin hydrolase	Lct	+∞	2,45E-05	2	1,3
Cell signalling						
P0C1X8; F1LRI7	AP2-associated protein kinase 1	Aak1	−∞	2,24E-05	3	4,6
D3ZAX5	Calcium homeostasis endoplasmic reticulum protein (Predicted)	Cherp	−∞	3,09E-05	3	4,5
D3ZHC4	Heme binding protein 2 (Predicted), isoform CRA_b	Hebp2	−∞	3,18E-08	3	17,7
G3V7J2; Q4V8C7	Interferon-inducible double-stranded RNA-dependent protein kinase activator A	Prkra	−∞	2,22E-03	4	21,1
A0A096MJY1	Protein Gpc6	Gpc6	−∞	7,43E-06	4	10,1
D3ZQC6	Protein Ubr1	Ubr1	−∞	1,04E-06	6	6,8
A0A0G2K2U5; D3ZUQ0	RILP-like protein 1	Rilpl1	−∞	8,30E-08	6	19,6
Q498D8	Ring-box 1, E3 ubiquitin protein ligase	Rbx1	−∞	9,57E-03	3	25
P84817	Mitochondrial fission 1 protein	Fis1	0,47	5,31E-04	5	42,1
F1LVV4	Regulator of chromosome condensation 2	Rcc2	0,80	9,83E-04	9	26
G3V9T7	ASNA1 ATPase	Asna1	0,82	8,11E-03	8	34,2
D3ZH75	AKT1 substrate 1 (Proline-rich) (Predicted), isoform CRA_d	Akt1s1	+∞	1,76E-04	3	19,1
P14668	Annexin A5	Anxa5	+∞	1,05E-05	1	7,8
Q62865	cGMP-inhibited 3,5-cyclic phosphodiesterase A	Pde3a	+∞	1,42E-04	2	2,9
B1WBY1	Cul1 protein	Cul1	+∞	1,50E-05	9	16,4
Q923V4	F-box only protein 6	Fbxo6	+∞	1,80E-06	4	16,5
P60517; Q0VGK0; P60522; F1M1J6; A0A0G2JU55	Gamma-aminobutyric acid receptor-associated protein	Gabarap	+∞	2,08E-10	2	15,4
Q91V33	KH domain-containing, RNA-binding, signal transduction-associated protein 1	Khdrbs1	+∞	8,12E-06	4	12
Q68FQ9	LanC lantibiotic synthetase component C-like 2	Lancl2	+∞	3,79E-05	4	14,4
Q6NX65	Programmed cell death protein 10	Pdcd10	+∞	3,12E-04	3	21,9
B0BN72	Protein FAM195B	Mcrip1	+∞	5,91E-04	3	41,2
Q3MIF1; G3V8E4	Protein Ubfd1	Ubfd1	+∞	2,07E-04	3	14,1
B2RZ96	Ubiquitin Conjugating Enzyme E2 R2	Ube2r2	+∞	1,21E-03	3	14,7
Lipid metabolism						
D3ZPU3; Q6P7R8	Very-long-chain 3-oxoacyl-CoA reductase	Hsd17b12	−∞	4,27E-06	2	10,3
Q5BK81	Prostaglandin reductase 2 (PTGR2)	Ptgr2	0,82	1,61E-03	8	40,2
B0BNM9	Glycolipid transfer protein	Gltp	+∞	8,71E-06	2	12,9
Nucleotide/phosphate metabolism						
Q920P6	Adenosine deaminase	Ada	−∞	2,66E-04	9	31,5
Q06647	ATP synthase subunit O, mitochondrial	Atp5o	−∞	2,89E-05	3	24,4
A0A0G2K478; D3ZDE4	Deoxyguanosine kinase (Predicted), isoform CRA_b	Dguok	−∞	8,29E-03	4	20,6
F7EPZ4	Protein Dis3	Dis3	−∞	7,04E-06	6	7,5
Protease						
P62198	26S protease regulatory subunit 8	Psmc5	0,77	2,38E-03	19	57,9
D3ZHQ1	Dipeptidylpeptidase 8 (Predicted), isoform CRA_a	Dpp8	+∞	1,04E-03	4	6,6
Q5PPG2; Q9R0J8	Legumain	Lgmn	+∞	1,82E-03	2	9,9
Q6AYR8	Secernin-2	Scrn2	+∞	2,33E-03	4	16,8
Protein folding						
B2GV92; P83868	Prostaglandin E synthase 3 (p23)	Ptges3	0,82	4,80E-03	8	51,2
Q52KJ9	Protein Tmx1	Tmx1	+∞	1,53E-04	4	20,5
Structural						
D3ZCI9	Protein Myl10	Myl10	-∞	2,59E-04	2	7,5
V9GZ85; P63259; A0A0G2K3K2	Actin, cytoplasmic 2	Actg1	1,08	6,86E-03	32	81,3
Q4QQS8	Nucleoporin 85 kDa	Nup85	1,95	4,38E-03	7	13,4
D4A1B2	Arpin protein	Arpin	+∞	7,01E-07	5	29,6
A0A0G2KAJ7	Collagen alpha-1(XII) chain	Col12a1	+∞	7,52E-04	8	4
Transcription/translation						
M0RA26; Q71TY3; P24051	40S ribosomal protein S27	Rps27	−∞	5,97E-06	2	25
Q9QYU2	Elongation factor Ts, mitochondrial	Tsfm	−∞	1,15E-04	5	30,2
Q6AYL5	Splicing factor 3B subunit 4	Sf3b4	−∞	4,05E-03	3	14,4
Q5RKI1; A0A0G2K8B7	Eukaryotic initiation factor 4 A–II	Eif4a2	0,67	3,36E-03	11	45
G3V6F5; Q8CGS5	Zinc phosphodiesterase ELAC protein 2	Elac2	0,81	6,78E-03	9	15,2
Q5M827	Pirin	Pir	0,85	2,49E-03	4	16,8
A0A0H2UHV4; M0R7Z0; B2GUV7	Eukaryotic translation initiation factor 5B	Eif5b	1,21	1,77E-03	12	15,2
A0A096MIS3; Q63186	Translation initiation factor eIF-2B subunit delta	Eif2b4	1,59	2,08E-03	6	19,6
P62250	40S ribosomal protein S16	Rps16	+∞	1,83E-03	5	32,9
G3 V992	General transcription factor II E, polypeptide 1 (alpha subunit)	Gtf2e1	+∞	1,24E-04	2	5,5

Table 1 (*continued*)

ID UniProtKB	Protein	Gene	PR-11/Control ratio	p value	Razor + unique peptides	Unique + razor coverage [%]
2 h						
B5DEK0	Regulation of nuclear pre-MRNA domain containing 1B	Rprd1b	+∞	1,85E-06	5	26,1
D3ZCD7; D3ZL21	TP53 regulating kinase	Tp53rk	+∞	3,74E-06	3	17,6
Other processes						
Q5BJP9	Phytanoyl-CoA dioxygenase domain-containing protein 1	Phyhd1	+∞	7,22E-03	7	36,1
Q6AYT5	Protein-glutamate *O*-methyltransferase	Armt1	+∞	2,32E-08	5	15,5
Q642A4	UPF0598 protein C8orf82 homolog	C8orf82	+∞	1,50E-04	2	14,2
6 h						
Carbohydrate metabolism						
D3ZY02	ATH1, Acid Trehalase-Like 1	Athl1	0,71	5,49E-03	8	16,6
Q5BJY6	*N*-acetylglucosamine-6-phosphate deacetylase	Amdhd2	+∞	2,96E-04	3	10,3
Cell signalling						
P0C1X8; F1LRI7	AP2-associated protein kinase 1	Aak1	−∞	1,85E-06	3	4,6
Q6P7Q1	BRCA1-A complex subunit BRE	Bre	−∞	2,83E-04	2	7,3
A0A0G2JYN0; Q5U2M6	DDB1- and CUL4-associated factor 8	Dcaf8	−∞	6,30E-03	6	15,9
F1LP57	Mitogen-Activated Protein Kinase Kinase 4	Map2k4	−∞	6,00E-04	3	11,6
Q5U204	Regulator complex protein LAMTOR3	Lamtor3	−∞	2,30E-04	3	37,1
G3V9H0; P50904	Ras GTPase-activating protein 1	Rasa1	−∞	1,59E-03	7	10,4
Q5HZY0	UBX domain-containing protein 4	Ubxn4	−∞	1,32E-03	2	6,9
D3ZCT7	Sec23 homolog B, coat complex II component	Sec23b	0,65	4,92E-04	10	18,5
A0A096MKH2; Q4KM55	Vesicle trafficking 1	Vta1	0,65	3,84E-03	7	30,7
P63245; A0A0G2JZE6	RACK1 (Receptor of activated protein C kinase 1)	Rack1	0,66	7,74E-04	15	68,5
G3V9S9	SEC24 homolog D, COPII coat complex component	Sec24d	0,66	1,91E-03	16	24,4
Q4KLJ8	PDCL3 (Phosducin-like protein 3)	Pdcl3	0,71	4,09E-03	6	27,9
Q4QQR9; F1LNE5	Protein MEMO1	Memo1	0,74	8,94E-03	14	75,8
Q68FW9	COP9 signalosome complex subunit 3	Cops3	0,84	8,38E-03	10	35,9
P35213	14–3-3 protein beta/alpha	Ywhab	1,46	5,14E-03	10	55,3
D3Z8L7	Ras-related protein R-Ras	Rras	1,48	3,85E-04	5	31,7
P97586; A0A0A0MXV3	CGR11 (cell growth regulatory gene 11 protein)	Cgref1	1,83	3,64E-04	4	19,9
F1LM60	ArfGAP With RhoGAP Domain, Ankyrin Repeat And PH Domain 1	Arap1	+∞	1,79E-04	4	4,7
Q712J3; Q496Z1	Bicaudal D homolog 2, isoform CRA_a	Bicd2	+∞	1,20E-04	7	10,9
O35826; A0A0G2K7T2	Bifunctional UDP-*N*-acetylglucosamine 2-epimerase/*N*-acetylmannosamine kinase	Gne	+∞	6,81E-03	7	15,2
G3V8Z9; F1MAA2	COP9 Signalosome Subunit 7 A	Cops7a	+∞	5,67E-03	5	25,8
G3V927; P97839	Discs, large homolog-associated protein 4	Dlgap4	+∞	1,59E-04	6	7,5
B4F7C7	Heme Binding Protein 1	Hebp1	+∞	1,75E-03	2	17,9
F1M9B2	Insulin-like growth factor binding protein 7, isoform CRA_b	Igfbp7	+∞	1,60E-04	4	23,5
Q91V33	KH domain-containing, RNA-binding, signal transduction-associated protein 1	Khdrbs1	+∞	8,08E-05	4	12
Q9QX69	LanC-like protein 1	Lancl1	+∞	1,07E-04	7	26,6
A0A0G2K0P2; O70436; G3 V603; O54835	Mothers against decapentaplegic homolog	Smad2	+∞	2,21E-04	2	5,8
A0A0G2K7P7; A0A0G2K459	Protein Mtch2	Mtch2	+∞	3,31E-04	3	22
Q5U1Z2	Trafficking protein particle complex subunit 3	Trappc3	+∞	1,67E-03	4	22,2
Lipid metabolism						
O88637	Ethanolamine-phosphate cytidylyltransferase	Pcyt2	+∞	5,38E-03	1	3,2
Q6IMY6; Q64194	Lysosomal acid lipase/cholesteryl ester hydrolase	Lipa	+∞	4,92E-04	3	11,6
Nucleotide/phosphate metabolism						
Q3MIE9	Spermine Synthase	Sms	+∞	1,02E-03	8	28,4
Protease						
Q6P9V7; Q63797	Proteasome activator complex subunit 1	Psme1	0,70	1,83E-03	14	50,2
Protein folding						
Q6AY58	B-cell receptor-associated protein 31	Bcap31	1,54	9,77E-03	3	11,4
P63036	DnaJ homolog subfamily A member 1	Dnaja1	+∞	1,01E-04	6	23,7
A0A0G2K093; O35162	Heat shock 70 kDa protein 13	Hspa13	+∞	1,23E-03	6	18,1
G3 V828	Protein Cnpy3	Cnpy3	+∞	3,28E-06	4	17
F1M8A5;	Protein Hypk	Hypk	+∞	9,18E-04	4	42,6
B2GUZ7	Tubulin Folding Cofactor C	Tbcc	+∞	1,31E-05	4	19,4
Structural						
P16636	Protein-lysine 6-oxidase	Lox	−∞	9,65E-03	2	8,3
A0A0G2K6B2; A0A0G2K1P8	TRIO And F-actin binding protein	Triobp	−∞	4,12E-03	8	15
A0A140TAG5; Q3KR86; A0A0G2JVH4	Mitochondrial inner membrane protein	Immt	0,65	2,23E-03	12	30,6
G3V6S0; A0A0G2K8W9; A0A0G2JZY6	Spectrin Beta, Non-Erythrocytic 1	Sptbn1	0,85	3,77E-03	80	44,7
Q5XFX0	Transgelin-2	Tagln2	1,25	9,77E-03	16	84,4

(*continued on next page*)

Table 1 (*continued*)

6 h						
ID UniProtKB	Protein	Gene	PR-11/Control ratio	p value	Razor + unique peptides	Unique + razor coverage [%]
B2GV74	Kinesin light chain 2 (Predicted), isoform CRA_b	Klc2	+∞	3,87E-04	4	9
B1WBY6; G3V6M8	Nucleoporin 37 kDa	Nup37	+∞	9,17E-03	4	18,8
Q66HC5	Nucleoporin 93 kDa	Nup93	+∞	4,83E-04	3	8,3
D3ZNS1; A0A0G2JV32; A0A0G2JTS5; Q63312	Pleckstrin homology-like domain family B member 1	Phldb1	+∞	4,97E-04	9	8,3
Transcription/translation						
A0A0G2JVA7; Q6VV72; B5DF60	Eukaryotic translation initiation factor 1 A	Eif1a	−∞	1,43E-04	3	21,5
Q5M965	Probable tRNA(His) guanylyltransferase	Thg1l	−∞	1,57E-04	3	14,4
G3V6S8	Serine/arginine-rich splicing factor 6	Srsf6	−∞	9,69E-04	6	15
X1WI37; P62703; A0A0H2UHX3; D3ZX01	40S ribosomal protein S4	Rps4x	0,75	4,14E-03	7	29,8
E9PST5	Acinus (apoptotic chromatin condensation inducer 1)	Acin1	0,75	6,40E-03	15	15,6
Q9JJ54	hnRPN D (heterogeneous nuclear ribonucleoprotein D0)	Hnrnpd	0,77	5,89E-03	13	34,6
B5DEN5	Eukaryotic translation elongation factor 1 beta 2	Eef1b2	0,81	9,69E-04	9	61,8
M0RA26; Q71TY3; P24051	40S ribosomal protein S27	Rps27	+∞	9,94E-07	2	25
B1WBQ0; O08837	CDC5L_RAT Cell division cycle 5-like protein	Cdc5l	+∞	3,47E-04	3	7
A0A0G2JTY6; F1LRK4	G-Rich RNA Sequence Binding Factor 1	Grsf1	+∞	3,78E-03	5	19,7
D3ZFB2	LUC7 Like 3 Pre-MRNA Splicing Factor	Luc7l3	+∞	1,70E-03	3	8,4
D3ZUL8	Zinc Finger CCHC-Type Containing 8	Zcchc8	+∞	3,60E-03	4	9,6
Other processes						
Q5XIT9	Methylcrotonoyl-CoA carboxylase beta chain, mitochondrial	Mccc2	−∞	5,88E-04	6	16,3
Q6AYT5	Protein-glutamate *O*-methyltransferase	Armt1	−∞	3,25E-04	5	15,5
B0K020	CDGSH iron-sulfur domain-containing protein 1	Cisd1	+∞	4,75E-03	2	25,9
A0A0G2K1N9	Selenoprotein O	Selo	+∞	1,04E-06	3	6,8
Q6AY72	UPF0449 protein C19orf25 homolog	C19orf25	+∞	9,36E-06	3	54,1
10 h						
Carbohydrate metabolism						
P43424	Galactose-1-phosphate uridylyltransferase	Galt	−∞	2,75E-05	3	9,5
Q02401; A9CMC8	Lactase-phlorizin hydrolase	Lct	+∞	2,13E-03	2	1,3
Cell signalling						
B5DFH4; A0A0G2K950	3′-Phosphoadenosine 5′-Phosphosulfate Synthase 2	Papss2	−∞	1,48E-04	3	6,2
P62332	ADP-ribosylation factor 6	Arf6	−∞	4,64E-04	3	24,6
B2RYJ3	Cullin 4 A	Cul4a	−∞	4,49E-04	6	9,2
D4A0W7	Fibronectin Type III Domain Containing 3B	Fndc3b	−∞	1,75E-03	7	8,5
Q562C6	Leucine zipper transcription factor-like protein 1	Lztfl1	−∞	1,06E-04	5	24,7
Q5BJX0	N-terminal Xaa-Pro-Lys *N*-methyltransferase 1	Ntmt1	−∞	2,05E-03	4	24,7
A0A0G2QC06; Q4FZX7	Signal recognition particle receptor subunit beta	Srprb	−∞	1,01E-05	9	11,2
Q5I0H3	Small ubiquitin-related modifier 1	Sumo1	−∞	1,97E-04	4	42,6
D4A6C6; A0A0U1RRU5	TGF-beta activated kinase 1/MAP3K7 binding protein 1	Tab1	−∞	6,46E-06	4	9,6
D3ZPR0	Exportin-2	Cse1l	0,56	8,28E-04	17	24,5
Q9ER24	Ataxin-10	Atxn10	0,57	8,58E-03	15	42,3
M0RA08	Perilipin	Plin3	0,61	3,76E-03	15	55,9
Q80U96	Exportin-1	Xpo1	0,63	2,93E-03	23	29,9
Q9EQX9	UBE2N (Ubiquitin-conjugating enzyme E2 N)	Ube2n	0,72	2,40E-03	7	65,1
A0A0G2K0X9; G3 V699; Q9Z2Q1	Protein transport protein Sec31A	Sec31a	0,73	4,24E-04	38	38,2
A1L1M0; P27791	PKA C-alpha (cAMP-dependent protein kinase catalytic subunit alpha)	Prkaca	0,74	4,99E-03	12	41,9
Q5U211	Sorting nexin-3	Snx3	0,74	9,60E-03	6	35,2
Q99J82	Integrin-linked protein kinase	Ilk	0,76	6,14E-03	9	21,9
Q5XI34	Protein Phosphatase 2 Regulatory Subunit A, Alpha	Ppp2r1a	0,78	6,51E-03	28	58,6
*F*1 M779; P11442	Clathrin heavy chain 1	Cltc	0,82	6,31E-03	77	57,3
P47875	Cysteine and glycine-rich protein 1	Csrp1	1,41	5,82E-03	10	60,1
F1M6A8; A0A0G2JXD7; Q63484	RAC-gamma serine/threonine-protein kinase	Akt3	+∞	1,58E-05	2	5,8
D4A511	Signal recognition particle 9 kDa protein	Srp9	+∞	1,06E-03	2	25,6
A0A0G2K2V2; G3V9N8; P52303	AP complex subunit beta	Ap1b1	+∞	5,33E-03	11	17,7
Lipid metabolism						
B0BNM9	Glycolipid transfer protein	Gltp	−∞	9,30E-04	2	12,9
F8WG67; Q64559	Cytosolic acyl coenzyme A thioester hydrolase	Acot7	0,81	6,57E-03	7	29,8
D3ZKG1	Methylmalonyl-CoA Mutase	Mut	+∞	8,12E-05	4	5,8
Nucleotide/phosphate metabolism						
D4A8A0	CAD trifunctional protein	Cad	0,78	8,45E-03	22	14,9
Protease						
Q99ML5	Prenylcysteine oxidase	Pcyox1	−∞	1,52E-04	6	19,4
Q07009	Calpain-2 catalytic subunit	Capn2	0,85	6,40E-03	36	61,1
P18420	Proteasome subunit alpha type-1	Psma1	1,26	2,07E-03	14	61,6
Structural						
Q08163	CAP1 (Adenylyl cyclase-associated protein 1)	Cap1	0,76	3,16E-03	26	73,6

Table 1 (*continued*)

10 h						
ID UniProtKB	Protein	Gene	PR-11/Control ratio	p value	Razor + unique peptides	Unique + razor coverage [%]
F1LN42	Tensin 1	Tns1	0,77	2,72E-03	31	27,9
D3ZU74; Q6AZ35; G3V9V3; Q62871	Cytoplasmic dynein 1 intermediate chain 2	Dync1i2	0,91	5,08E-03	19	48,2
G3 V624	Coronin 1C	Coro1c	1,19	8,98E-05	16	38,4
D4AC70	Collagen Type VIII Alpha 1	Col8a1	+∞	5,75E-03	4	6,7
A0A0G2K2Z0; F1LT71	Echinoderm microtubule associated protein like 4	Eml4	+∞	1,11E-07	3	4,5
F1LYQ8	FERM, RhoGEF and pleckstrin domain-containing protein 1	Farp1	+∞	6,59E-06	5	5,6
Transcription/translation						
Q04931	FACT complex subunit SSRP1	Ssrp1	−∞	1,03E-06	6	10
D3ZFB2	LUC7 like 3 pre-MRNA splicing factor	Luc7l3	−∞	2,89E-03	3	8,4
D4AE49	Ski2 Like RNA Helicase 2	Skiv2l2	−∞	6,89E-04	6	7
Q5M7V8	Thyroid hormone receptor-associated protein 3	Thrap3	−∞	2,27E-04	10	13,7
D4A720	SFRS7 (serine/arginine-rich splicing factor 7)	Srsf7	1,17	6,97E-03	7	28,6
Q5XI97	Alanyl-tRNA editing protein Aarsd1	Aarsd1	+∞	7,78E-03	4	15
G3V8Y5	DNA-directed RNA polymerase subunit beta	Polr2b	+∞	2,82E-03	7	8,5
D3ZZ62	Exportin, tRNA (Nuclear export receptor for tRNAs) (Predicted), isoform CRA_a	Xpot	+∞	4,63E-05	6	10
D4A7F2	Protein Mycbp	Mycbp	+∞	4,54E-06	4	55,3
Q4QR99; A0A0H2UHF3	Queuine tRNA-ribosyltransferase	Qtrt1	+∞	3,48E-04	3	10,2
P86252; F1LPS8	Transcriptional activator protein Pur-alpha (Fragments)	Pura	+∞	3,33E-03	3	42
Other processes						
G3V8P2; Q8VHT6	Arsenite methyltransferase	As3mt	−∞	1,67E-03	2	8,4
D3ZSR7	Protein Ccdc102a	Ccdc102a	−∞	5,51E-04	4	10
D3ZII8	SMYD Family Member 5	Smyd5	−∞	1,08E-04	3	12
B4F7E0; Q2A121; A0A0G2K675	Alpha-ketoglutarate-dependent dioxygenase FTO	Fto	0,66	2,95E-03	9	27,1
A0A0G2JY07	Minichromosome maintenance complex component 5 (CDC46)	Mcm5	0,71	6,17E-03	10	18,8
D3ZIE9	Aldehyde Dehydrogenase 18 Family Member A1	Aldh18a1	0,85	2,77E-03	32	53,1
D3Z8Q7	Protein Fam96b	Fam96b	+∞	2,12E-03	2	26,1
Q6AYT5	Protein-glutamate *O*-methyltransferase	Armt1	+∞	2,01E-03	5	15,5

Ratio > 1 corresponds to an increase in abundance, whereas < 1 indicates decreased levels. Proteins identified only in untreated cells or exposed fibroblasts are marked as fold infinity (±).

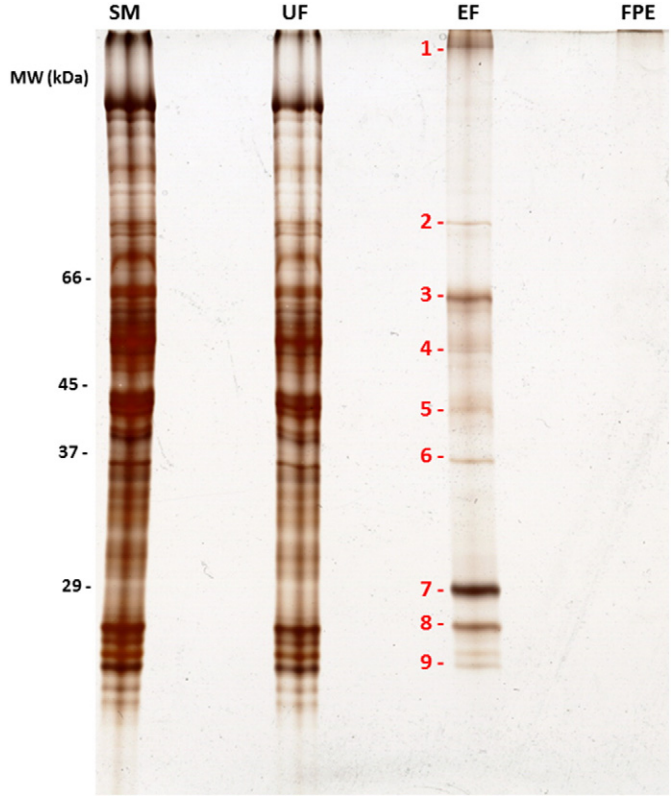

Fig. 4. 12% SDS-PAGE analysis of the immobilized PR-11 affinity chromatography. SM: starting material; UF: unbound fraction; EF: eluted fraction; FPE: fraction prior to elution. The specific displacement is shown by eluted fraction at low concentration of PR-11 (50 μM) and absence of unbound proteins at fraction prior to elution. Identified proteins in eluted fraction are in Table 2. Silver staining.

(vascular endothelial growth factor) and its receptor (VEGFR-1) [14]. In this context, at 6 h exposure we found decreased expression of RACK1 (receptor for activated C kinase), which mediates ubiquitin-dependent proteasomal degradation of HIF-1α [26], consequently allowing for sustained cellular levels of this factor to favour angiogenesis. Our findings also revealed downregulation of hnRPN D (heterogenous nuclear ribonucleoprotein D), which is in agreement with the angiogenic effects of PR-11. Overexpression of hnRPN D in macrophages leads to decreased levels of endogenous VEGF, through its binding to the 3´-UTR of VEGF mRNA [27]. We also hypothesize that the angiogenic promoting effects of PR-11 are unlikely associated to VEGFR-2 activation. At least two observations in this study support this hypothesis: downregulated levels of PDCL3 (phosducin-like 3) and increased expression of R-ras. The former is a chaperone whose activity is associated to high expression levels of VEGFR-2 [28,29], whilst R-ras is a signalling molecule that prevents internalization of this receptor [30].

- Nuclear factor kappa B pathway

The NF-κB protein family members are transcription factors responsible for regulation of expression of several genes, including those encoding cytokines and plasma membrane receptors. Therefore, their roles in both innate and adaptive immune responses as well as in inflammatory processes have been established [31,32]. In particular, abolishing proteasomal degradation of IκB, an inhibitor of NF-κB, by the peptides PR-11 and PR-39 leads to decreased expression of NF-κB dependent pro-inflammatory proteins such as VCAM-1 (vascular cell adhesion molecule-1) and ICAM-1 (intercellular adhesion molecule-1) [15,16]. In this context, after 10 h exposure we found lower levels of PKA C-alpha, a catalytic subunit of protein kinase A, involved in *in vitro* activation and nuclear translocation of NF-κB in unstimulated murine cells [33]. Corroborating this finding, at the same time point decreased levels of ILK (integrin-linked kinase) [34] and UBE2N (a ubiquitin-conjugating

Table 2
PR-11 binding proteins recovered by affinity chromatography.

Band	ID UniProtKB	Protein name	Gene name	% coverage	Peptides (unique)	% relative area detector	MW [kDa]
1	P07756	Carbamoyl-phosphate synthase [ammonia], mitochondrial	Cps1	16,9	19 (19)	34,0	164,5
	P48721	Stress-70 protein, mitochondrial	Hspa9	27,7	13 (13)	20,4	73,8
	P04762	Catalase	Cat	19,9	8 (8)	20,0	59,7
	P00884	Fructose-bisphosphate aldolase B	Aldob	12,6	3 (3)	10,9	39,6
2	P06761	78 kDa glucose-regulated protein	Hspa5	47,1	30 (28)	73,1	72,3
	P48721	Stress-70 protein, mitochondrial	Hspa9	29,5	14 (14)	23,2	73,8
3	P02770	Serum albumin	Alb	56,6	32 (32)	51,6	68,7
	P04762	Catalase	Cat	45,9	20 (20)	21,7	59,7
4	P10719	ATP synthase subunit beta, mitochondrial	Atp5b	36,7	14 (14)	20,2	56,3
	P04764	Alpha-enolase	Eno1	46,3	12 (12)	15,3	47,1
	P18418	Calreticulin	Calr	9,6	3 (3)	10,9	48,0
5	P00507	Aspartate aminotransferase, mitochondrial	Got2	9,5	3 (3)	58,8	47,3
	O09171	Betaine–homocysteine *S*-methyltransferase 1	Bhmt	10,6	3 (3)	41,2	44,9
6	P00481	Ornithine carbamoyltransferase, mitochondrial	Otc	39,8	12 (12)	71,4	39,9
	P07824	Arginase-1	Arg1	26,3	7 (7)	10,8	35,0
7	O35796	Complement component 1 Q subcomponent-binding protein, mitochondrial	C1qbp	31,9	5 (5)	96,2	31,0
8	P14141	Carbonic anhydrase 3	Ca3	54,6	10 (10)	65,7	29,4
	P04904	Glutathione S-transferase alpha-3	Gsta3	18,6	4 (4)	17,3	25,3
9	P08010	Glutathione S-transferase Mu 2	Gstm2	61,9	16 (16)	44,0	25,7
	P04905	Glutathione S-transferase Mu 1	Gstm1	45,4	13 (13)	31,4	25,9
	O35244	Peroxiredoxin-6	Prdx6	56,7	11 (11)	17,2	24,8

Relative area detector (%) was obtained by dividing the area of given protein by the total area detected for all proteins identified in that band.

enzyme) [35] were also detected, giving further evidences of negative regulation of the NF-κB pathway through distinct mechanisms.

There is only one published work describing the effects of the PR-11 peptide to culture cells [36]. The authors have demonstrated decreased expression of VCAM-1 in endothelial cells exposed to 1 μM PR-11. The cells were previously stimulated with TNF- α and the protein VCAM-1 detected by western blotting. Although this protein has not been identified as differentially expressed in our study, other three proteins whose transcription is NF-κB dependent were found to be differentially expressed (*e.g.*, PKA C-alpha, ILK and UBE2N) in agreement with the anti-inflammatory effect attributed to the PR-11 peptide.

Differentially expressed proteins shown to have a role in oncogenesis were found for the three timing points. At 2 h, decreased levels of ASNA1, prostaglandin E synthase 3 (p23) and prostaglandin reductase 2 (PTGR2) were observed. Reduced expression of ASNA1, an ATPase required to insertion of tail-anchored proteins to the endoplasmic reticulum, is associated to inhibition of cell growth and increased apoptosis in melanoma cells [37]. The co-chaperone p23 is a subunit of the Hsp90 complex shown to be upregulated in several cancers, mainly in metastatic cells [38–40]. As for the prostaglandin E2 metabolism, the knockdown of PTGR2 suppressed cell growth and induced apoptosis in gastric cancer [41]. At 6 h post exposure, downregulation of MEMO1 (mediator of ErbB2-driven cell motility 1) also suggests a role for PR-11 in interfering with cell motility. Overexpression of MEMO1 has been associated to aggressiveness and increased potential for metastasis in pancreatic and mammary gland cell lines [42,43]. Lower levels of CAP1 (adenylyl cyclase-dependent protein 1) and exportin-1 (XPO-1) were found at 10 h exposure. CAP1 is a structural and highly conserved molecule involved in regulation of actin filaments [44]. Knocking down expression of CAP1 through RNAi inhibited proliferation and cell migration in three cancer cell models [45–47]. XPO-1 is tightly linked to cell-cycle regulation by mediating the nucleus to cytoplasm transportation of proteins such as those encoded by tumour suppressor genes [48]. In fact, overexpression of XPO-1 has been associated to different cancer types such as leukemias, gliomas and osteosarcomas [49–51]. Altogether, our findings potentially highlight novel biological properties of PR-11 that could be of interest to cancer research.

Our final approach aimed the identification of PR-11 interacting proteins by means of affinity chromatography using the immobilized peptide. After stringent washing steps, PR-11 bound proteins were selectively eluted using soluble PR-11. One out of nine protein bands appeared significantly enriched in a 1-D gel separation as revealed by silver staining. This particular protein (band 7) was identified as gC1qR (complement component 1, q subcomponent binding protein), an acid glycoprotein able to bind with high affinity to the globular portion of complement C1q [52]. This protein is reported to be found in distinct cell compartments such as mitochondria, nucleus and membranes of various cell types [53–55] and its function has been related to growth and survival of many tumour models [56]. More recently, Agemy et al. (2013) identified gC1qR as a ligand and transporter of the positively charged peptide CGKRK, which shares structural similarity to the N-terminal portion of PR-11, coupled to a pro-apoptotic drug in breast cancer models. Once bound to surface gC1qR, the complex is internalized to the mitochondria where the drug is released [57]. In agreement to our findings, it has previously been reported that PR-39 is easily taken up by fibroblasts, possibly by a receptor ligand exposed on the cell membrane [21]. Given the noticeable enrichment of gC1qR as a target of PR-11 in our affinity approach, here we provide preliminary evidence of gC1qR mediating the interaction and internalization of this peptide.

The remaining eight putative PR-11 ligands, all found at vanishingly small amounts, deserve further investigation to discriminate genuine from unspecific interaction with PR-11. Anyhow, the identification of two urea cycle components (ornithine carbamoyltransferase and arginase-1) might indicate that those enzymes are capable to interact with peptides rich in proline and arginine residues. This possible interaction remains to be conclusively demonstrated. In corroboration with our findings, a recent report revealed *E. coli* proteins related to the metabolism of arginine and ornithine as ligands of PR-39 using a microarray approach [58].

Various proteins known to reduce the cellular oxidative stress were also co-eluted (*e.g.*, catalase, peroxiredoxin-6 and glutathione S-transferase isoforms). It was previously demonstrated that the PR-39 peptide decrease the production of superoxide radicals through binding and inhibition of NADPH oxidase [13]. In this context, our findings suggest a similar role for the PR-11 peptide broadening its anti-inflammatory properties.

5. Conclusion

Here we aimed to provide the first inventory of proteomic alterations caused by exposure of cultured fibroblasts to the PR-11 peptide. Proteins

that appeared significantly altered were dependent on the timing of exposure and were predominantly related to signalling, transcription and translation. Of note, our data revealed proteins involved with the HIF-1α and NF-κB being altered, highlighting the capabilities of PR-11 to interfere with inflammatory processes and favour angiogenesis.

Supplementary data to this article can be found online at http://dx.doi.org/10.1016/j.bbapap.2016.09.017.

Transparency document

The Transparency document associated with this article can be found, in online version.

Acknowledgements

This work was financially supported by 'Fundação de Amparo à Pesquisa do Estado de Minas Gerais' (FAPEMIG, grant numbers APQ-01503/09 and APQ-00950/12) and 'Coordenação de Aperfeiçoamento de Pessoal de Nível Superior' (CAPES). GSB was a recipient of a CAPES scholarship for the funding during his MSc degree in Biotechnology and PhD degree in Biological Sciences. Authors also acknowledge the Mass Spectrometry Laboratory at Brazilian Biosciences National Laboratory, CNPEM, Campinas, Brazil for their initial support in this project.

References

[1] B. Agerberth, J.Y. Lee, T. Bergman, M. Carlquist, H.G. Boman, V. Mutt, H. Jornvall, Amino acid sequence of PR-39. Isolation from pig intestine of a new member of the family of proline-arginine-rich antibacterial peptides, Eur. J. Biochem. FEBS 202 (1991) 849–854.
[2] P. Storici, M. Zanetti, A cDNA derived from pig bone marrow cells predicts a sequence identical to the intestinal antibacterial peptide PR-39, Biochem. Biophys. Res. Commun. 196 (1993) 1058–1065.
[3] C.M. Linde, S.E. Hoffner, E. Refai, M. Andersson, In vitro activity of PR-39, a proline-arginine-rich peptide, against susceptible and multi-drug-resistant Mycobacterium tuberculosis, J. Antimicrob. Chemother. 47 (2001) 575–580.
[4] B. Ramanathan, E.G. Davis, C.R. Ross, F. Blecha, Cathelicidins: microbicidal activity, mechanisms of action, and roles in innate immunity, Microbes Infect. 4 (2002) 361–372.
[5] H.G. Boman, B. Agerberth, A. Boman, Mechanisms of action on *Escherichia coli* of cecropin *P*1 and PR-39, two antibacterial peptides from pig intestine, Infect. Immun. 61 (1993) 2978–2984.
[6] M. Scocchi, A. Tossi, R. Gennaro, Proline-rich antimicrobial peptides: converging to a non-lytic mechanism of action, Cell. Mol. Life Sci. 68 (2011) 2317–2330.
[7] H.J. Huang, C.R. Ross, F. Blecha, Chemoattractant properties of PR-39, a neutrophil antibacterial peptide, J. Leukoc. Biol. 61 (1997) 624–629.
[8] B. Ramanathan, H. Wu, C.R. Ross, F. Blecha, PR-39, a porcine antimicrobial peptide, inhibits apoptosis: involvement of caspase-3, Dev. Comp. Immunol. 28 (2004) 163–169.
[9] J. Wu, C. Parungo, G. Wu, P.M. Kang, R.J. Laham, F.W. Sellke, M. Simons, J. Li, PR39 inhibits apoptosis in hypoxic endothelial cells: role of inhibitor apoptosis protein-2, Circulation 109 (2004) 1660–1667.
[10] C.R. Ross, G. Ricevuti, A.I. Scovassi, The antimicrobial peptide PR-39 has a protective effect against HeLa cell apoptosis, Chem. Biol. Drug Des. 70 (2007) 154–157.
[11] T. Ohtake, Y. Fujimoto, K. Ikuta, H. Saito, M. Ohhira, M. Ono, Y. Kohgo, Proline-rich antimicrobial peptide, PR-39 gene transduction altered invasive activity and actin structure in human hepatocellular carcinoma cells, Br. J. Cancer 81 (1999) 393–403.
[12] K. Tanaka, Y. Fujimoto, M. Suzuki, Y. Suzuki, T. Ohtake, H. Saito, Y. Kohgo, PI3-kinase p85alpha is a target molecule of proline-rich antimicrobial peptide to suppress proliferation of ras-transformed cells, Jpn. J. Cancer Res. 92 (2001) 959–967.
[13] J. Shi, C.R. Ross, T.L. Leto, F. Blecha, PR-39, a proline-rich antibacterial peptide that inhibits phagocyte NADPH oxidase activity by binding to Src homology 3 domains of p47 phox, Proc. Natl. Acad. Sci. U. S. A. 93 (1996) 6014–6018.
[14] J. Li, M. Post, R. Volk, Y. Gao, M. Li, C. Metais, K. Sato, J. Tsai, W. Aird, R.D. Rosenberg, T.G. Hampton, F. Sellke, P. Carmeliet, M. Simons, PR39, a peptide regulator of angiogenesis, Nat. Med. 6 (2000) 49–55.
[15] Y. Gao, S. Lecker, M.J. Post, A.J. Hietaranta, J. Li, R. Volk, M. Li, K. Sato, A.K. Saluja, M.L. Steer, A.L. Goldberg, M. Simons, Inhibition of ubiquitin-proteasome pathway-mediated I kappa B alpha degradation by a naturally occurring antibacterial peptide, J. Clin. Invest. 106 (2000) 439–448.
[16] J. Bao, K. Sato, M. Li, Y. Gao, R. Abid, W. Aird, M. Simons, M.J. Post, PR-39 and PR-11 peptides inhibit ischemia-reperfusion injury by blocking proteasome-mediated I kappa B alpha degradation, Am. J. Physiol. Heart Circ. Physiol. 281 (2001) H2612–H2618.
[17] M. Gaczynska, P.A. Osmulski, Y. Gao, M.J. Post, M. Simons, Proline- and arginine-rich peptides constitute a novel class of allosteric inhibitors of proteasome activity, Biochemistry 42 (2003) 8663–8670.
[18] C.A. Luber, J. Cox, H. Lauterbach, B. Fancke, M. Selbach, J. Tschopp, S. Akira, M. Wiegand, H. Hochrein, M. O'Keeffe, M. Mann, Quantitative proteomics reveals subset-specific viral recognition in dendritic cells, Immunity 32 (2010) 279–289.
[19] I. Matsumoto, Y. Mizuno, N. Seno, Activation of Sepharose with epichlorohydrin and subsequent immobilization of ligand for affinity adsorbent, J. Biochem. 85 (1979) 1091–1098.
[20] U.K. Laemmli, Cleavage of structural proteins during the assembly of the head of bacteriophage T4, Nature 227 (1970) 680–685.
[21] Y.R. Chan, R.L. Gallo, PR-39, a syndecan-inducing antimicrobial peptide, binds and affects p130(Cas), J. Biol. Chem. 273 (1998) 28978–28985.
[22] Q. Hu, R.J. Noll, H. Li, A. Makarov, M. Hardman, R. Graham Cooks, The Orbitrap: a new mass spectrometer, J. Mass Spectrom. 40 (2005) 430–443.
[23] N. Nagaraj, N.A. Kulak, J. Cox, N. Neuhauser, K. Mayr, O. Hoerning, O. Vorm, M. Mann, System-wide perturbation analysis with nearly complete coverage of the yeast proteome by single-shot ultra HPLC runs on a bench top Orbitrap, Mol. Cell. Proteomics 11 (2012) (M111 013722).
[24] E.D. Muinck, N. Nagy, D. Tirziu, M. Murakami, N. Gurusamy, S.K. Goswami, S. Ghatpande, R.M. Engelman, M. Simons, D.K. Das, Protection against myocardial ischemia-reperfusion injury by the angiogenic Masterswitch protein PR 39 gene therapy: the roles of HIF1alpha stabilization and FGFR1 signaling, Antioxid. Redox Signal. 9 (2007) 437–445.
[25] D. Tirziu, E. Chorianopoulos, K.L. Moodie, R.T. Palac, Z.W. Zhuang, M. Tjwa, C. Roncal, U. Eriksson, Q. Fu, A. Elfenbein, A.E. Hall, P. Carmeliet, L. Moons, M. Simons, Myocardial hypertrophy in the absence of external stimuli is induced by angiogenesis in mice, J. Clin. Invest. 117 (2007) 3188–3197.
[26] Y.V. Liu, J.H. Baek, H. Zhang, R. Diez, R.N. Cole, G.L. Semenza, RACK1 competes with HSP90 for binding to HIF-1alpha and is required for O(2)-independent and HSP90 inhibitor-induced degradation of HIF-1alpha, Mol. Cell 25 (2007) 207–217.
[27] A. Fellows, M.E. Griffin, B.L. Petrella, L. Zhong, F.P. Parvin-Nejad, R. Fava, P. Morganelli, R.B. Robey, R.C. Nichols, AUF1/hnRNP D represses expression of VEGF in macrophages, Mol. Biol. Cell 23 (2012) 1414–1422.
[28] S. Srinivasan, R.D. Meyer, R. Lugo, N. Rahimi, Identification of PDCL3 as a novel chaperone protein involved in the generation of functional VEGF receptor 2, J. Biol. Chem. 288 (2013) 23171–23181.
[29] S. Srinivasan, V. Chitalia, R.D. Meyer, E. Hartsough, M. Mehta, I. Harrold, N. Anderson, H. Feng, L.E. Smith, Y. Jiang, C.E. Costello, N. Rahimi, Hypoxia-induced expression of phosducin-like 3 regulates expression of VEGFR-2 and promotes angiogenesis, Angiogenesis 18 (2015) 449–462.
[30] J. Sawada, F. Li, M. Komatsu, R-ras inhibits VEGF-induced p38MAPK activation and HSP27 phosphorylation in endothelial cells, J. Vasc. Res. 52 (2015) 347–359.
[31] M.S. Hayden, S. Ghosh, NF-kappaB in immunobiology, Cell Res. 21 (2011) 223–244.
[32] K. Iwai, Diverse roles of the ubiquitin system in NF-kappaB activation, Biochim. Biophys. Acta 1843 (2014) 129–136.
[33] F. Shirakawa, S.B. Mizel, In vitro activation and nuclear translocation of NF-kappa B catalyzed by cyclic AMP-dependent protein kinase and protein kinase C, Mol. Cell. Biol. 9 (1989) 2424–2430.
[34] F. Liang, S. Zhang, B. Wang, J. Qiu, Y. Wang, Overexpression of integrin-linked kinase (ILK) promotes glioma cell invasion and migration and down-regulates E-cadherin via the NF-kappaB pathway, J. Mol. Histol. 45 (2014) 141–151.
[35] M. Pulvino, Y. Liang, D. Oleksyn, M. DeRan, E. Van Pelt, J. Shapiro, I. Sanz, L. Chen, J. Zhao, Inhibition of proliferation and survival of diffuse large B-cell lymphoma cells by a small-molecule inhibitor of the ubiquitin-conjugating enzyme Ubc13-Uev1A, Blood 120 (2012) 1668–1677.
[36] A. Anbanandam, D.C. Albarado, D.C. Tirziu, M. Simons, S. Veeraraghavan, Molecular basis for proline- and arginine-rich peptide inhibition of proteasome, J. Mol. Biol. 384 (2008) 219–227.
[37] O. Hemmingsson, Y. Zhang, M. Still, P. Naredi, ASNA1, an ATPase targeting tail-anchored proteins, regulates melanoma cell growth and sensitivity to cisplatin and arsenite, Cancer Chemother. Pharmacol. 63 (2009) 491–499.
[38] E. Oxelmark, J.M. Roth, P.C. Brooks, S.E. Braunstein, R.J. Schneider, M.J. Garabedian, The cochaperone p23 differentially regulates estrogen receptor target genes and promotes tumor cell adhesion and invasion, Mol. Cell. Biol. 26 (2006) 5205–5213.
[39] N.E. Simpson, W.M. Lambert, R. Watkins, S. Giashuddin, S.J. Huang, E. Oxelmark, R. Arju, T. Hochman, J.D. Goldberg, R.J. Schneider, L.F. Reiz, F.A. Soares, S.K. Logan, M.J. Garabedian, High levels of Hsp90 cochaperone p23 promote tumor progression and poor prognosis in breast cancer by increasing lymph node metastases and drug resistance, Cancer Res. 70 (2010) 8446–8456.
[40] L.Q. Cano, D.N. Lavery, S. Sin, E. Spanjaard, G.N. Brooke, J.D. Tilman, A. Abroaf, L. Gaughan, C.N. Robson, R. Heer, F. Mauri, J. de Rooij, K. Driouch, C.L. Bevan, The co-chaperone p23 promotes prostate cancer motility and metastasis, Mol. Oncol. 9 (2015) 295–308.
[41] E.Y. Chang, S.H. Tsai, C.T. Shun, S.W. Hee, Y.C. Chang, Y.C. Tsai, J.S. Tsai, H.J. Chen, J.W. Chou, S.Y. Lin, L.M. Chuang, Prostaglandin reductase 2 modulates ROS-mediated cell death and tumor transformation of gastric cancer cells and is associated with higher mortality in gastric cancer patients, Am. J. Pathol. 181 (2012) 1316–1326.
[42] R. Marone, D. Hess, D. Dankort, W.J. Muller, N.E. Hynes, A. Badache, Memo mediates ErbB2-driven cell motility, Nat. Cell Biol. 6 (2004) 515–522.
[43] T. Kalinina, C. Gungor, S. Thieltges, M. Moller-Krull, E.M. Penas, D. Wicklein, T. Streichert, U. Schumacher, V. Kalinin, R. Simon, B. Otto, J. Dierlamm, H. Schwarzenbach, K.E. Effenberger, M. Bockhorn, J.R. Izbicki, E.F. Yekebas, Establishment and characterization of a new human pancreatic adenocarcinoma cell line with high metastatic potential to the lung, BMC Cancer 10 (2010) 295.
[44] A.V. Hubberstey, E.P. Mottillo, Cyclase-associated proteins: CAPacity for linking signal transduction and actin polymerization, FASEB J. 16 (2002) 487–499.

[45] K. Yamazaki, M. Takamura, Y. Masugi, T. Mori, W. Du, T. Hibi, N. Hiraoka, T. Ohta, M. Ohki, S. Hirohashi, M. Sakamoto, Adenylate cyclase-associated protein 1 overexpressed in pancreatic cancers is involved in cancer cell motility, Lab. Investig. 89 (2009) 425–432.
[46] Y. Liu, X. Cui, B. Hu, C. Lu, X. Huang, J. Cai, S. He, L. Lv, X. Cong, G. Liu, Y. Zhang, R. Ni, Upregulated expression of CAP1 is associated with tumor migration and metastasis in hepatocellular carcinoma, Pathol. Res. Pract. 210 (2014) 169–175.
[47] X.F. Yu, Q.C. Ni, J.P. Chen, J.F. Xu, Y. Jiang, S.Y. Yang, J. Ma, X.L. Gu, H. Wang, Y.Y. Wang, Knocking down the expression of adenylate cyclase-associated protein 1 inhibits the proliferation and migration of breast cancer cells, Exp. Mol. Pathol. 96 (2014) 188–194.
[48] K. Stade, C.S. Ford, C. Guthrie, K. Weis, Exportin 1 (Crm1p) is an essential nuclear export factor, Cell 90 (1997) 1041–1050.
[49] B. Falini, C. Mecucci, E. Tiacci, M. Alcalay, R. Rosati, L. Pasqualucci, R. La Starza, D. Diverio, E. Colombo, A. Santucci, B. Bigerna, R. Pacini, A. Pucciarini, A. Liso, M. Vignetti, P. Fazi, N. Meani, V. Pettirossi, G. Saglio, F. Mandelli, F. Lo-Coco, P.G. Pelicci, M.F. Martelli, G.A.L.W. Party, Cytoplasmic nucleophosmin in acute myelogenous leukemia with a normal karyotype, N. Engl. J. Med. 352 (2005) 254–266.
[50] A. Shen, Y. Wang, Y. Zhao, L. Zou, L. Sun, C. Cheng, Expression of CRM1 in human gliomas and its significance in p27 expression and clinical prognosis, Neurosurgery 65 (2009) 153–159 (discussion 159-160).
[51] Y. Yao, Y. Dong, F. Lin, H. Zhao, Z. Shen, P. Chen, Y.J. Sun, L.N. Tang, S.E. Zheng, The expression of CRM1 is associated with prognosis in human osteosarcoma, Oncol. Rep. 21 (2009) 229–235.
[52] B. Ghebrehiwet, B.L. Lim, E.I. Peerschke, A.C. Willis, K.B. Reid, Isolation, cDNA cloning, and overexpression of a 33-kD cell surface glycoprotein that binds to the globular "heads" of C1q, J. Exp. Med. 179 (1994) 1809–1821.
[53] T. Muta, D. Kang, S. Kitajima, T. Fujiwara, N. Hamasaki, p32 protein, a splicing factor 2-associated protein, is localized in mitochondrial matrix and is functionally important in maintaining oxidative phosphorylation, J. Biol. Chem. 272 (1997) 24363–24370.
[54] B.J. Soltys, D. Kang, R.S. Gupta, Localization of *P*32 protein (gC1q-R) in mitochondria and at specific extramitochondrial locations in normal tissues, Histochem. Cell Biol. 114 (2000) 245–255.
[55] M. Majumdar, J. Meenakshi, S.K. Goswami, K. Datta, Hyaluronan binding protein 1 (HABP1)/C1QBP/p32 is an endogenous substrate for MAP kinase and is translocated to the nucleus upon mitogenic stimulation, Biochem. Biophys. Res. Commun. 291 (2002) 829–837.
[56] F.R. Dembitzer, Y. Kinoshita, D. Burstein, R.G. Phelps, M.B. Beasley, R. Garcia, N. Harpaz, S. Jaffer, S.N. Thung, P.D. Unger, B. Ghebrehiwet, E.I. Peerschke, gC1qR expression in normal and pathologic human tissues: differential expression in tissues of epithelial and mesenchymal origin, J. Histochem. Cytochem. 60 (2012) 467–474.
[57] L. Agemy, V.R. Kotamraju, D. Friedmann-Morvinski, S. Sharma, K.N. Sugahara, E. Ruoslahti, Proapoptotic peptide-mediated cancer therapy targeted to cell surface p32, Mol. Ther. 21 (2013) 2195–2204.
[58] Y.H. Ho, P. Shah, Y.W. Chen, C.S. Chen, Systematic analysis of intracellular-targeting antimicrobial peptides, Bactenecin 7, hybrid of Pleurocidin and Dermaseptin, proline-arginine-rich peptide, and Lactoferricin B, by using *Escherichia coli* proteome microarrays, Mol. Cell. Proteomics 15 (2016) 1837–1847.